Received: 3 May 2019 | Revised: 12 February 2020 | Accepted: 10 March 2020

DOI: 10.1111/bph.15057

Themed Issue: Pulmonary hypertension and right heart failure: new therapeutic avenue/approaches

RESEARCH PAPER

Amelioration of elastase-induced lung emphysema and reversal of pulmonary hypertension by pharmacological iNOS inhibition in mice

Athanasios Fysikopoulos[1] | Michael Seimetz[1] | Stefan Hadzic[1] | Fenja Knoepp[1] | Cheng-Yu Wu[1] | Kathrin Malkmus[1] | Jochen Wilhelm[1] | Alexandra Pichl[1] | Mariola Bednorz[1] | Elsa Tadele Roxlau[1] | Hossein A. Ghofrani[1] | Natascha Sommer[1] | Mareike Gierhardt[3] | Ralph T. Schermuly[1] | Werner Seeger[1,2] | Friedrich Grimminger[1] | Norbert Weissmann[1] | Simone Kraut[1]

[1]Justus-Liebig University of Giessen (JLUG), Excellence Cluster Cardiopulmonary Institute (CPI), Universities of Giessen and Marburg Lung Center (UGMLC), Member of the German Center for Lung Research (DZL), Giessen, Germany

[2]Max Planck Institute for Heart and Lung Research, Bad Nauheim, Germany

[3]Max-Planck Heart and Lung Laboratory, Instituto de Investigación en Biomedicina de Buenos Aires (IBioBA)—CONICET—Partner Institute of the Max Planck Society, Buenos Aires, Argentina

Correspondence
Norbert Weissmann, Excellence Cluster Cardiopulmonary Institute (CPI), Aulweg 130, D-35392 Giessen, Germany.
Email: norbert.weissmann@innere.med.uni-giessen.de

Funding information
Deutsche Forschungsgemeinschaft, Grant/Award Number: 268555672

Background and Purpose: Chronic obstructive pulmonary disease, encompassing chronic airway obstruction and lung emphysema, is a major worldwide health problem and a severe socio-economic burden. Evidence previously provided by our group has shown that inhibition of inducible NOS (iNOS) prevents development of mild emphysema in a mouse model of chronic tobacco smoke exposure and can even trigger lung regeneration. Moreover, we could demonstrate that pulmonary hypertension is not only abolished in cigarette smoke-exposed iNOS$^{-/-}$ mice but also precedes emphysema development. Possible regenerative effects of pharmacological iNOS inhibition in more severe models of emphysema not dependent on tobacco smoke, however, are hitherto unknown.

Experimental Approach: We have established a mouse model using a single dose of porcine pancreatic elastase or saline, intratracheally instilled in C57BL/6J mice. Emphysema, as well as pulmonary hypertension development was determined by both structural and functional measurements.

Key Results: Our data revealed that (i) emphysema is fully established after 21 days, with the same degree of emphysema after 21 and 28 days post instillation, (ii) emphysema is stable for at least 12 weeks and (iii) pulmonary hypertension is evident, in contrast to smoke models, only after emphysema development. Oral treatment with the iNOS inhibitor N(6)-(1-iminoethyl)-L-lysine (L-NIL) was started after emphysema establishment and continued for 12 weeks. This resulted in significant

Abbreviations: COPD, chronic obstructive pulmonary disease; GOLD, global initiative for chronic obstructive lung disease; iNOS, inducible NOS; L-NIL, N(6)-(1-iminoethyl)-L-lysine; LV, left ventricle; MLI, mean linear intercept; ONOO−, peroxynitrite; PBGD, porphobilinogen deaminase; PH, pulmonary hypertension; PPE, porcine pancreatic elastase; RV, right ventricle; RVSP, right ventricular systolic pressure; S, Septum.

Athanasios Fysikopoulos, Michael Seimetz, Norbert Weissmann and Simone Kraut have equal contribution.

lung regeneration, evident in the improvement of emphysema and reversal of pulmonary hypertension.

Conclusion and Implications: Our data indicate that iNOS is a potential new therapeutic target to treat severe emphysema and associated pulmonary hypertension.

LINKED ARTICLES: This article is part of a themed issue on Risk factors, comorbidities, and comedications in cardioprotection. To view the other articles in this section visit http://onlinelibrary.wiley.com/doi/10.1111/bph.v178.1/issuetoc

1 | INTRODUCTION

Chronic obstructive pulmonary disease (COPD) is one of the leading causes of death worldwide and, according to the World Health Organization, estimated to become the third cause of death by 2030. Despite the extensive efforts that have been made, the disease remains still incurable due to lack of therapeutic targets that can prevent the development or even reverse the already established disease. Smoking cessation can only slow down the decline of forced expiratory volume in 1 s (FEV_1; Bohadana, Nilsson, Westin, Martinet, & Martinet, 2006) and pharmacological therapy may alleviate symptoms, but simultaneously negative effects of COPD-associated co-morbidities may occur (Kankaanranta et al., 2015). Thus, COPD causes high morbidity, mortality, disability and, besides the loss of life quality for the patients, a large socio-economic burden (Cazzola, Donner, & Hanania, 2007).

One of the major components of COPD is emphysema, defined by Snider, Kleinerman, Thurlbeck, and Bengali (1985) "a condition of the lung characterized by abnormal, permanent enlargement of airspaces distal to the terminal bronchiole, accompanied by the destruction of their walls, and without obvious fibrosis". Emphysema occurs secondary to airway remodelling or after the destruction of the alveoli due to exposure to noxious particles and gases, which cigarette smoke and smoke from biomass heating and indoor cooking being the most prominent sources (Sangani & Ghio, 2011).

Moreover, approximately 30%–70% of COPD patients suffer from pulmonary hypertension (PH; Girard et al., 2015). Although most patients show only borderline increased mean pulmonary arterial pressures (Minai, Chaouat, & Adnot, 2010), their morbidity is increased (Elwing & Panos, 2008). Thus, new insights into COPD-associated pulmonary hypertension are needed to understand the pathogenesis of this co-morbidity.

Our group has previously demonstrated the importance of **iNOS**, a **NO**-producing enzyme, in a mouse model of cigarette smoke-induced COPD/emphysema and pulmonary hypertension. Intriguingly, pulmonary hypertension preceded emphysema development in this model (Seimetz et al., 2011). We found iNOS to be up-regulated predominantly in the vasculature of smoke-exposed mice and COPD patients (GOLD IV). Inhibition of iNOS not only protected against tobacco smoke-induced emphysema and pulmonary hypertension but also mediated lung regeneration and reversed remodelling of the vasculature in this model. Moreover, we could show that under smoking conditions NO produced excessively by iNOS results in protein nitration, most probably via $ONOO^-$ formation from the reaction of NO with superoxide (Beckman, Beckman, Chen, Marshall, & Freeman, 1990; Pryor & Squadrito, 1995) (Dijkstra et al., 1998), which we suggested promoted alveolar destruction and lung vascular alterations.

However, since there are other causes for the development of emphysema than smoke exposure and as tobacco smoke exposure in mice resulted in only mild emphysema, we now aimed (i) to characterize the development of severe emphysema after a single-dose instillation of porcine pancreatic elastase (PPE), an enzyme that degrades the elastic fibres of the lung, (ii) to determine the time course of possible pulmonary hypertension development in elastase-induced emphysema and (iii) to study the effect of iNOS inhibition on established smoke-independent severe emphysema. Most importantly, we have chosen to apply a therapeutic approach i.e. giving the drug after full establishment of the disease to decipher possible regenerative effects.

Accordingly, animals were orally treated with the specific iNOS inhibitor L-NIL (N(6)-(1-iminoethyl)-L-lysine) after establishment of emphysema at a dosage shown to exert a highly selective inhibition of iNOS. We hypothesized that inhibition of iNOS in this mouse model would have a curative effect on both emphysema and pulmonary hypertension.

What is already known

- Oral application of the iNOS inhibitor L-NIL reverses mild, smoke-induced pulmonary hypertension and emphysema.

What this study adds

- Single application of elastase results in emphysema and pulmonary hypertension, concomitant with vascular remodelling.
- iNOS inhibition improves severe elastase-induced emphysema and reverses pulmonary hypertension.

What is the clinical significance

- iNOS inhibitors are potential candidates for the treatment of established, severe emphysema.

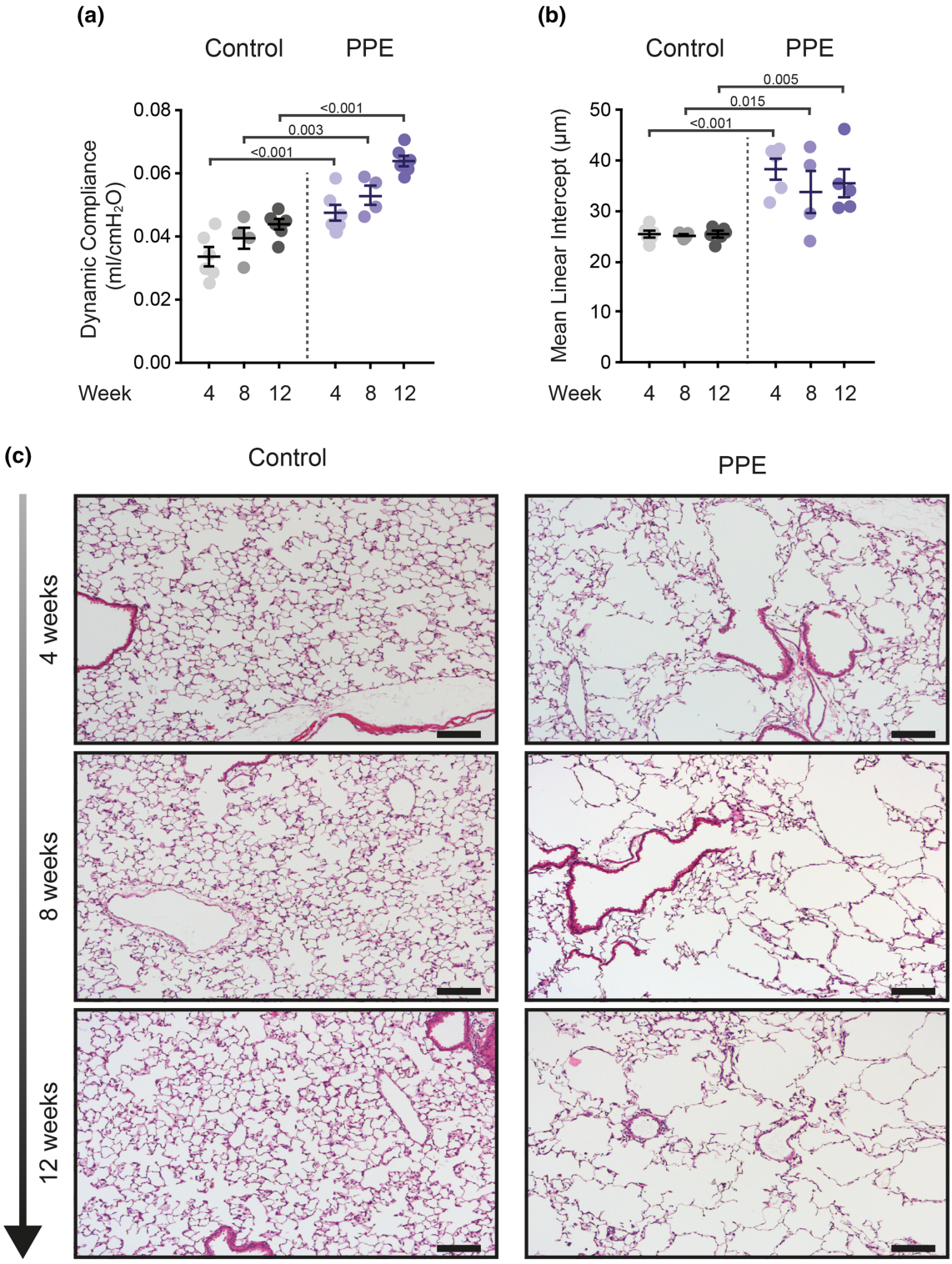

FIGURE 1 Characterization of emphysema development in mice 4, 8 and 12 weeks after porcine pancreatic elastase (PPE) instillation. Mice received either saline (control) or PPE and were investigated 4, 8 and 12 weeks after instillation. (a) *In vivo* dynamic lung compliance (control 4 weeks $n = 6$, PPE 4 weeks $n = 6$, control 8 weeks $n = 4$, PPE 8 weeks, $n = 4$, control 12 weeks $n = 6$, PPE 12 weeks n = 6). (b) Mean linear intercept (control 4 weeks $n = 6$, PPE 4 weeks $n = 5$, control 8 weeks $n = 5$, PPE 8 weeks, $n = 4$, control 12 weeks $n = 6$, PPE 12 weeks $n = 5$). (c) Representative histological images of lungs from all groups stained with haematoxylin/eosin staining. Scale bar indicates 100 µm

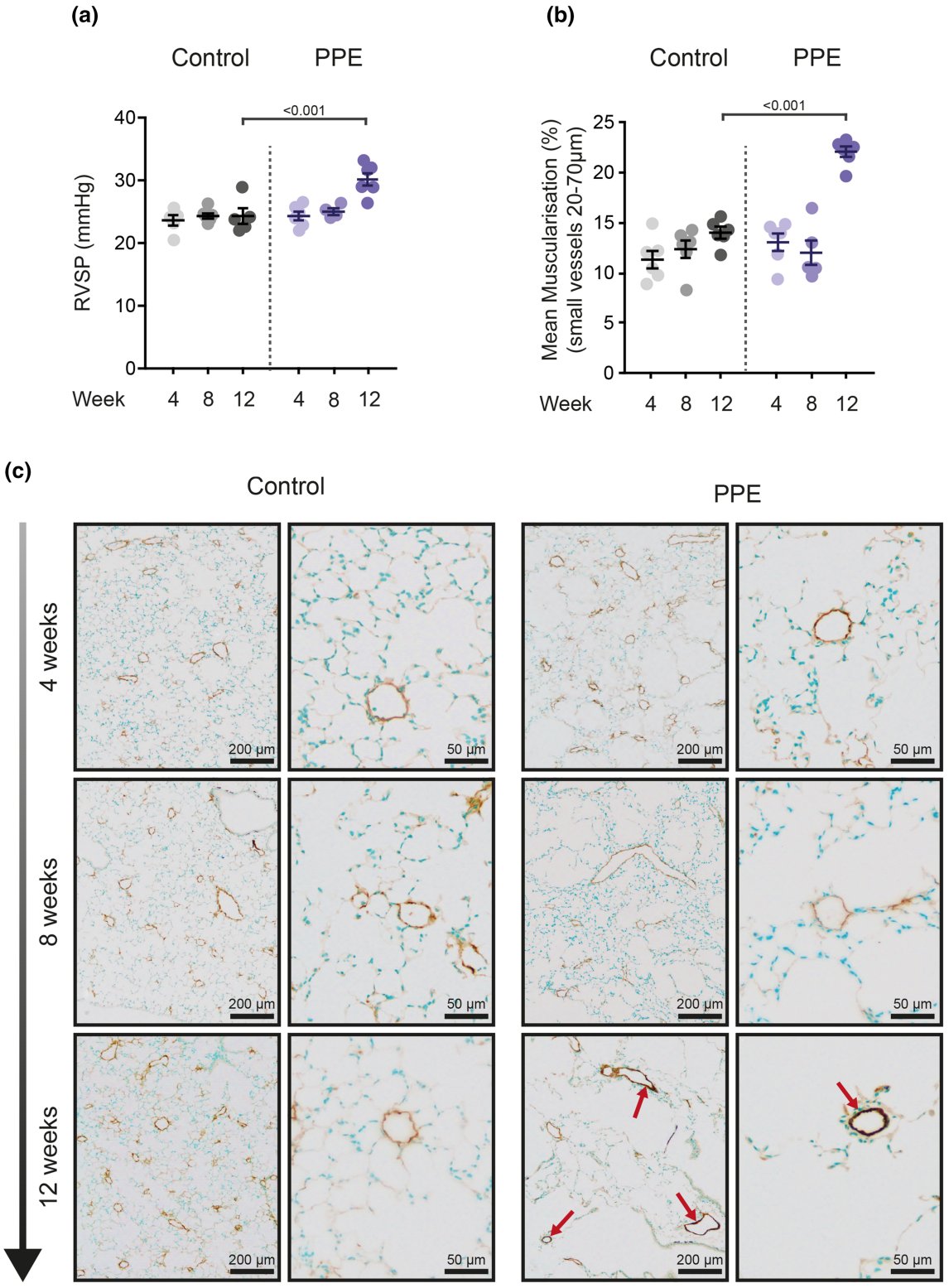

FIGURE 2 Characterization of pulmonary hypertension (PH) development in mice 4, 8 and 12 weeks after porcine pancreatic elastase (PPE) instillation. Mice received either saline (control) or PPE and were investigated 4, 8 and 12 weeks after instillation. (a) Right ventricular systolic pressure (RVSP; control 4 weeks $n = 5$, PPE 4 weeks $n = 6$, control 8 weeks $n = 6$, PPE 8 weeks, $n = 4$, control 12 weeks $n = 5$, PPE 12 weeks $n = 6$). (b) Mean muscularization of small pulmonary vessels (20–70 µm) ($n = 6$, each group except PPE 8 weeks $n = 5$). (c) Representative histological images of lungs from all groups stained against α-smooth muscle actin and von Willebrand factor. Red arrows are indicating fully muscularized vessels

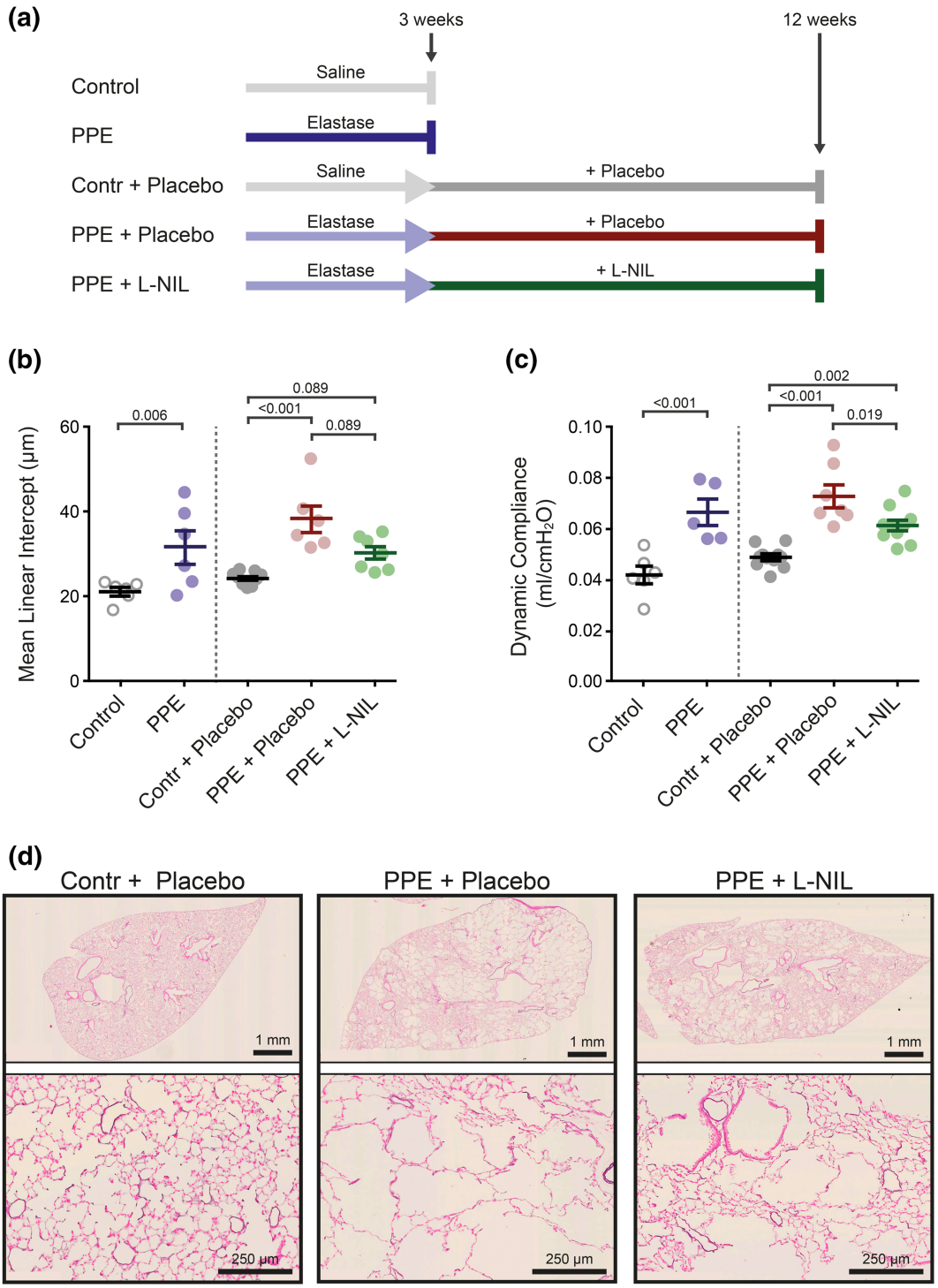

FIGURE 3 Effect of the iNOS inhibitor N(6)-(1-iminoethyl)-L-lysine (L-NIL) on elastase-induced emphysema, lung structural and functional assessment. Three weeks after instillation of porcine pancreatic elastase (PPE), mice were either killed and examined (PPE group) or received L-NIL (PPE + L-NIL group) or placebo (water, PPE + placebo group) for 3 months via the drinking water, whereas controls received sterile saline (control group) and placebo (water, control + placebo group). (a) Study design of the curative approach: (i) healthy control (saline, no L-NIL treatment, 3 weeks after saline application, $n = 6$), (ii) diseased control (PPE, investigation after induction of emphysema 3 weeks after instillation, $n = 6$), (iii) healthy aging control (control + placebo, 15 weeks after saline application $n = 13$), (iv) diseased aging control (PPE + placebo, 15 weeks after PPE application, $n = 13$) and (v) L-NIL-treated mice (PPE + L-NIL, 15 weeks after PPE application $n = 12$). (b) Mean linear intercept (control $n = 6$, PPE $n = 6$, control + placebo $n = 9$, PPE + placebo $n = 6$ and PPE + L-NIL $n = 7$). (c) *In vivo* dynamic lung compliance (control $n = 6$, PPE $n = 5$, control + placebo $n = 11$, PPE + placebo $n = 7$ and PPE + L-NIL $n = 10$). (d) Representative histological images stained with haematoxylin/eosin

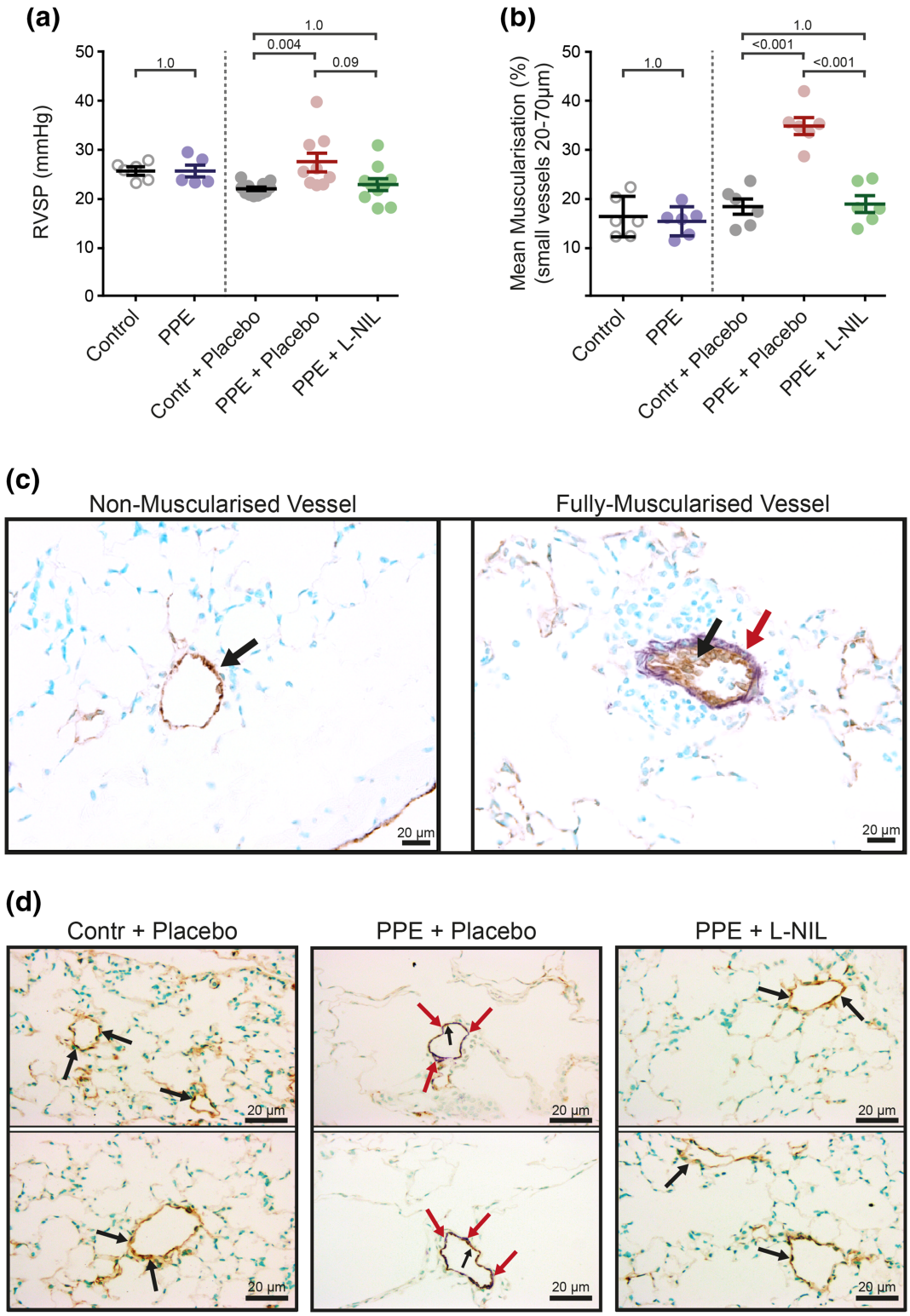

FIGURE 4 Treatment with N(6)-(1-iminoethyl)-L-lysine (L-NIL) reverses pulmonary hypertension (PH) development and vascular remodelling. Three weeks after instillation of saline or porcine pancreatic elastase (PPE), mice were either killed and examined (control and PPE) or received L-NIL (PPE + L-NIL) or placebo (water, PPE + placebo) for 3 months via the drinking water, whereas controls received sterile saline and placebo (water; control + placebo). At the end of the treatment period, haemodynamic parameters, right ventricular hypertrophy and vascular morphometry were assessed. (a) RVSP (control $n = 6$, PPE $n = 5$, control + placebo $n = 12$, PPE + placebo $n = 9$ and PPE + L-NIL $n = 10$) and (b) mean muscularization of small pulmonary vessels (20–70 µm, $n = 6$ for each group). (c,d) Representative histological images stained against α-smooth muscle actin and von Willebrand factor. Red arrows are indicating cells stained against α-smooth muscle actin (violet) and black arrows against von Willebrand factor (brown)

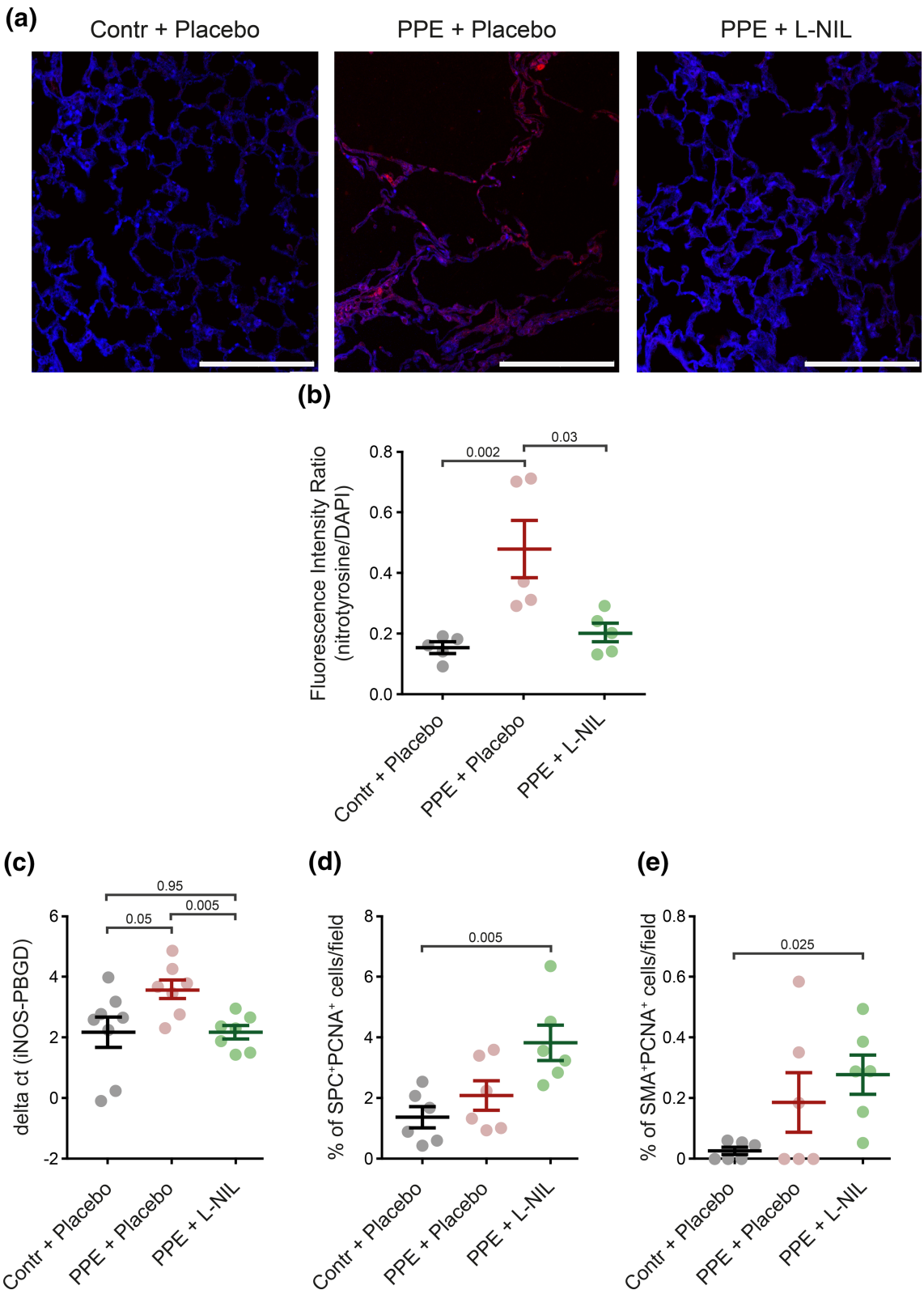

FIGURE 5 Effect of iNOS inhibition on 3-nitrotyrosine expression, *iNOS* gene expression and proliferation. (a) Representative images and (b) quantification of an immunofluorescence staining targeting nitrotyrosine in control (control + placebo), water-treated (porcine pancreatic elastase (PPE)+ placebo) and N(6)-(1-iminoethyl)-L-lysine (L-NIL)-treated (PPE + L-NIL) mice. The fluorescence intensity was normalized to DAPI, $n = 5$ per group. Scale bar indicates 150 μm. (c) Expression of *iNOS* in lung homogenate of control ($n = 8$), water-treated (PPE + placebo, $n = 7$) and L-NIL-treated (PPE + L-NIL, $n = 7$) mice. (d,e) Quantification of immunofluorescence staining for the proliferation marker PCNA in mouse lungs treated with either water (PPE + placebo, $n = 6$) or L-NIL (PPE + L-NIL, $n = 6$) as well as healthy controls (control + placebo, $n = 6$) for (d) surfactant protein C (SPC)-positive cells and (e) smooth muscle actin (SMA)-positive cells

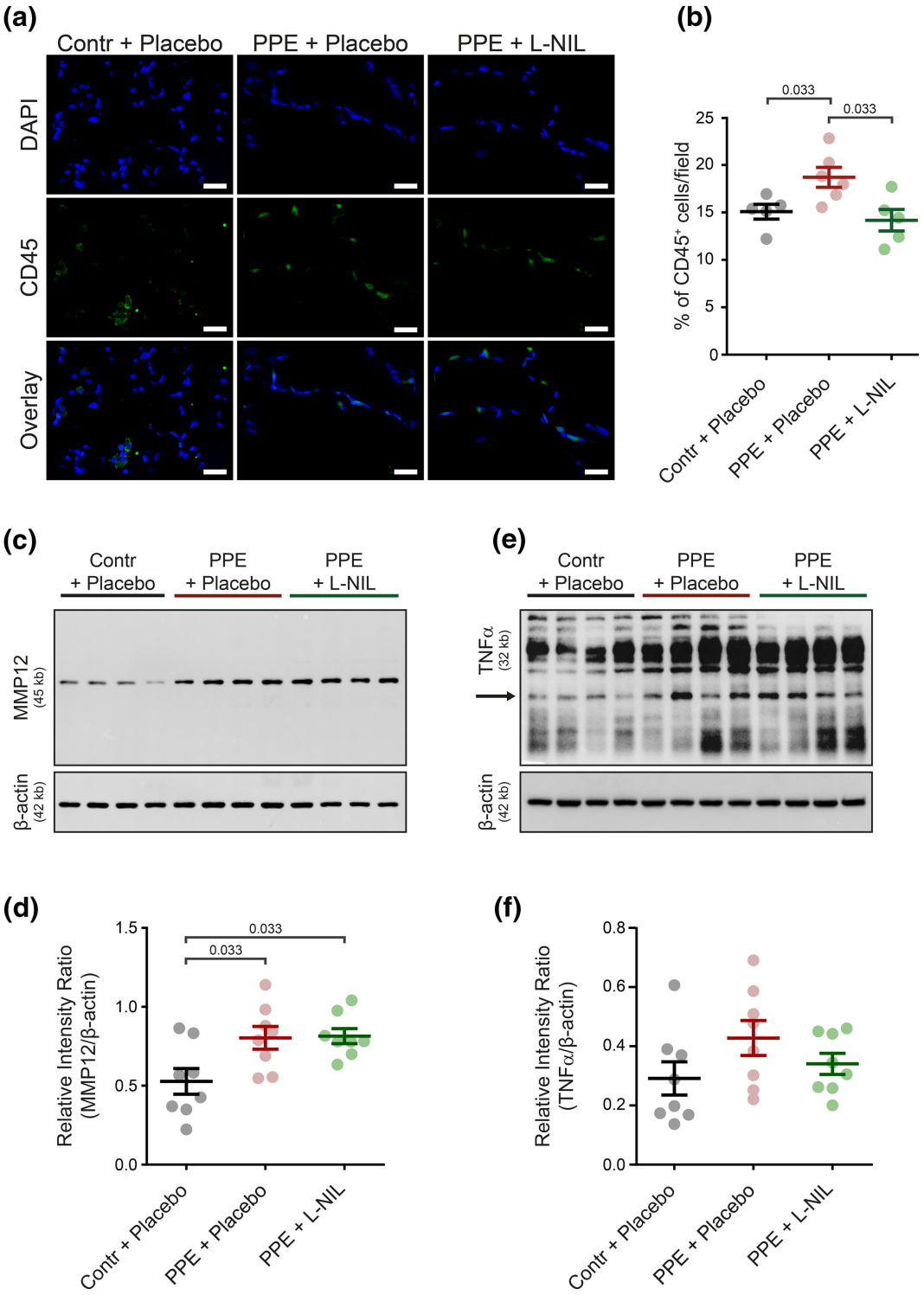

FIGURE 6 Effect of iNOS inhibition on inflammation. (a) Representative images and (b) quantification of immunofluorescence staining for inflammatory (CD45 positive) cells. The percentage of $CD45^+$ cells per field was quantified in control (control + placebo, $n = 5$), water-treated (porcine pancreatic elastase (PPE) + placebo, $n = 6$) and N(6)-(1-iminoethyl)-L-lysine (L-NIL)-treated (PPE + L-NIL, $n = 5$) mice. Scale bar indicates 25 μm. (c) Representative blot of MMP12 (45 kb) and (d) densitometric analysis. Data were normalized to β-actin (42 kb), $n = 8$ for each group. (e) Representative blot of TNF-α (32 kb) and (f) densitometric analysis. Data were normalized to β-actin (42 kb), $n = 8$ for each group

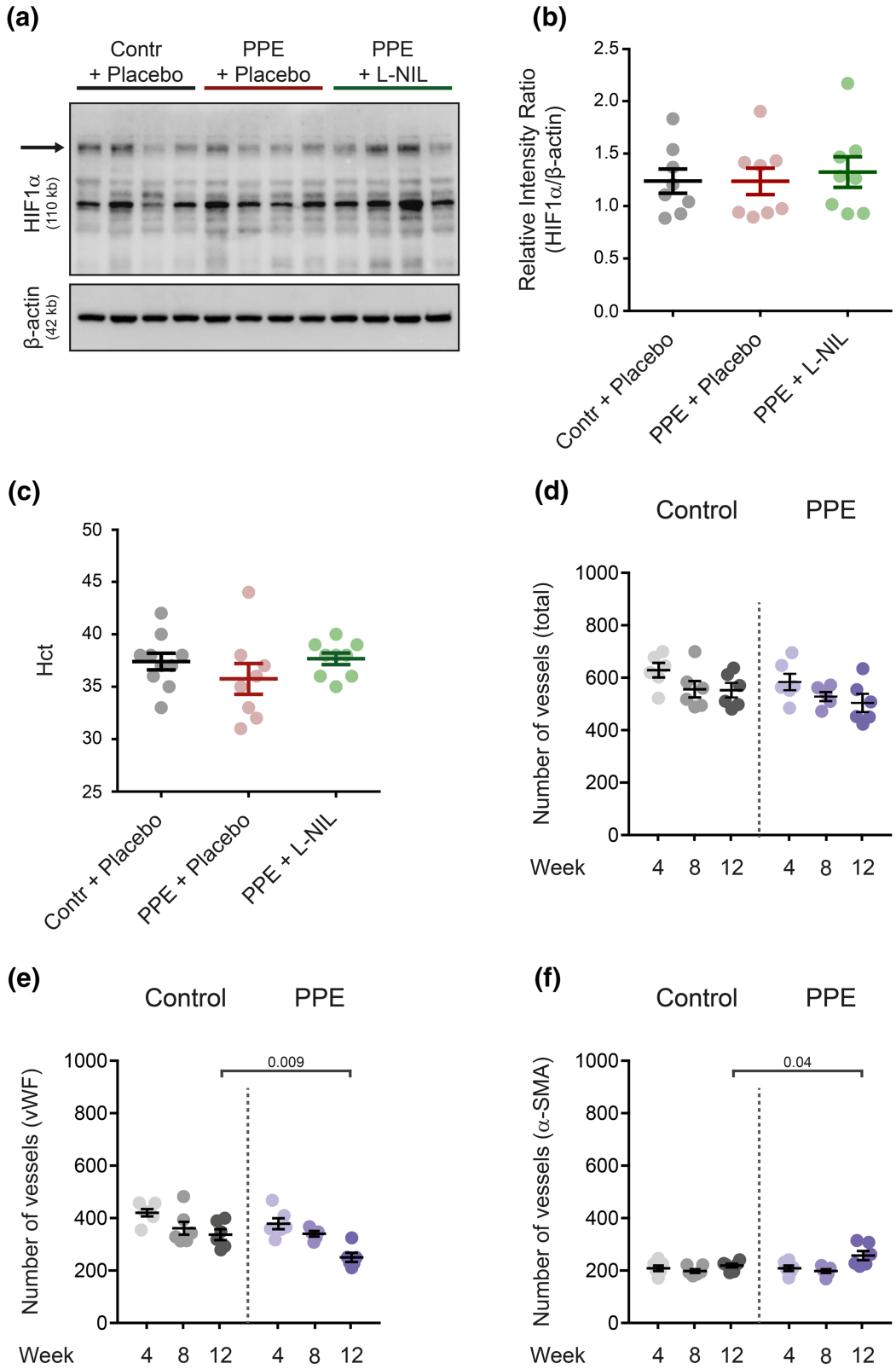

FIGURE 7 Hypoxia does not drive pulmonary hypertension (PH) upon elastase application. Mice received either N(6)-(1-iminoethyl)-L-lysine (L-NIL) (porcine pancreatic elastase (PPE) + L-NIL), placebo (water, PPE + placebo) or sterile saline (control + placebo) for 3 months. (a) Representative blot of hypoxia inducible factor (HIF)1α (110 kb) and (b) densitometric analysis. Data were normalized to β-actin (42 kb), $n = 8$ for each group. (c) At the end of the treatment period, haematocrit was analysed for control + placebo ($n = 10$), PPE + placebo ($n = 8$) and PPE + L-NIL ($n = 9$). (d–f) Amount of vessels in mice receiving either saline (control) or porcine pancreatic elastase (PPE), investigated 4, 8 and 12 weeks ($n = 6$, respectively, except 8 weeks PPE $n = 5$) after elastase instillation for (d) the total number of vessels, (e) the von Willebrand factor stained vessels and (f) the α-smooth muscle actin positive vessels. *F* was not significant for (b), (c) and (d)

2 | METHODS

All experiments were approved by the regional board (RP Giessen, Hesse, Germany; Az: V 54-19 c 20 15 h 01 GI 20/10 Nr. 54/2013) in accordance with the German animal welfare law and the European legislation for the protection of animals used for scientific purposes (2010/63/EU), as well as in accordance with local regulations and the NRC Guide for the Care and Use of Laboratory Animals followed at IBioBA-CONICET and approved by the local Institutional Animal Care and Use Committee (Comisión Institucional de Cuidado y Uso de Animales de Laboratorio; CICUAL) with the number 121 'New therapeutic approaches for pulmonary emphysema therapy by targeting iNOS' intending to establish an elastase model reducing the burden for the mice according to the 3R principle of Russell and Burch (1959). Estimation of group size was performed via sample size using Sigma Stat 3.5 (Systat Software Inc., San Jose, USA) with a power of 0.800 and an α of 0.05. For comparison of (i) two groups (comparing porcine pancreatic elastase (PPE) vs. control, Figures 1–4), dynamic compliance was used as a marker with difference in means of 0.02 and an SD of 0.011 (group size estimation was $n = 6$) and (ii) three groups (considering the pulmonary hypertension and treatment effect, Figures 3–7) right ventricular systolic pressure (RVSP) was used as a marker with difference in means of 5.901 and an SD of 3.774 (group size estimation was $n = 9$).

2.1 | Animals

Male C57BL/6J (Charles River, Sulzfeld, Germany), 8–10 weeks of age and 20–22 g of weight were used in the study. Animals were kept under controlled conditions (12 h dark/12 h light cycle, water and food supply *ad libitum*). For the characterization of the emphysema mouse model, either porcine pancreatic elastase or placebo (saline) was instilled intratracheally after randomization and mice were investigated 4, 8 and 12 weeks ($n = 6$ respectively) post instillation. In the 8 weeks porcine pancreatic elastase group, two of the mice died before the end of the experiment, resulting in $n = 4$ for this group.

For the curative treatment approach, mice were randomized and divided into the following groups, as illustrated in Figure 3a: (i) healthy controls (saline, no L-NIL treatment, 3 weeks after saline application), (ii) diseased controls (porcine pancreatic elastase (PPE), investigation after induction of emphysema 3 weeks after instillation), (iii) healthy aging controls (control + placebo, 15 weeks after saline application), (iv) diseased aging controls (PPE + placebo, 15 weeks after PPE application) and (v) L-NIL-treated mice (PPE + L-NIL, 15 weeks after PPE application). For this approach, six mice have been investigated for Groups 1 and 2 and 13 for Groups 3 to 5. For controls, sterile saline was either used as placebo or vehicle (for the elastase and water for the L-NIL administration. The degree of emphysema development was confirmed histologically by a blinded operator. Animal studies are reported in compliance with the ARRIVE guidelines (Kilkenny, Browne, Cuthill, Emerson, & Altman, 2010) and with the recommendations made by the *British Journal of Pharmacology*.

2.2 | Elastase

Porcine pancreatic elastase (ET947, Elastin Products Company, USA) was intratracheally instilled into mice at a dose of 2.4 U/100 g body weight. For the dose calculation and the preparation of the solutions, the specific activity of the enzyme was measured according to the recommendation and protocol of the manufacturer (Elastin Products Company, USA). Elastase was dissolved in sterile saline, and the mice received one single dose by intratracheal instillation according to the protocol described below.

2.3 | Anaesthesia and elastase treatment

Prior to intubation, the animals were anaesthetized with a mixture of 5% isoflurane gas (Baxter) in room air supplemented with 100% oxygen. During application, mice were monitored at all times and onset of surgical anaesthesia was assured by loss of the pedal reflex. Afterwards, the animals were placed on a mounting support and anaesthesia was maintained via a custom-made facemask (2-ml syringe) using 3%–4% isoflurane in oxygen supplement. After the displacement of the tongue, the intubation tube (intravenous catheter, Neoflon outer sheath, 20G × 11/4″, 33 mm length, B. Braun, Germany) was carefully inserted into the trachea; 100 µl of the elastase solution or sterile saline (healthy controls) followed by 200 µl of air was instilled through the endotracheal tube, using a 1-ml syringe attached to a small-diameter catheter (Neoflon outer sheath, 24G, 19 mm length; Becton Dickinson, Sweden). Establishment of emphysema was evident after 21 days post instillation.

2.4 | iNOS inhibitor treatment

The iNOS inhibitor L-NIL (N(6)-(1-iminoethyl)-L-lysine, dihydrochloride, Cayman chemical) or placebo (drinking water) was applied via the drinking water. For the inhibitor, a concentration (600 $\mu g \cdot ml^{-1} \triangleq 2.68$ mM) was used which was previously shown to be highly selective for iNOS without causing adverse effects in mice (Stenger, Thuring, Rollinghoff, Manning, & Bogdan, 1995). Mice with established emphysema were treated for 3 months with either L-NIL or placebo and were subsequently subjected to lung functional, haemodynamic and structural measurements.

2.5 | Lung function tests, *in vivo* haemodynamics

The mice were initially anaesthetized in a chamber using 5% isoflurane in oxygen supplement and maintained via a mask (3%–4% isoflurane in oxygen supplement) on a thermoregulating plate. Before intubation, the surgical tolerance of the anaesthesia was tested using the toe pinch withdrawal reflex. Afterwards, mice were connected to a FlexiVent FX system (SCIREQ, Montreal, Canada) allowing evaluation of the lung by the FlexiWare 7 software with a predefined script

provided by the manufacturer and a ventilation rate of 150 breaths·min^{-1}, a tidal volume of 5 ml·kg^{-1} as well as a positive end-expiratory pressure (PEEP) of 3 cmH_2O. After adaptation to the system, the script for measuring lung function was run following the manufacturer's recommendation with anaesthesia maintained at a concentration of 1.5%–2.5% isoflurane in oxygen supplement. The main parameter selected for the evaluation of lung function was dynamic compliance. An average of three measurements was used for every calculation and the quality of the measurement was determined by the system as a coefficient of at least 0.95. Only values above this coefficient were included in this study.

After assessment of lung function, haemodynamic measurements were performed. To this end, the right jugular vein and carotid artery were surgically prepared, and a Millar catheter (MIKRO-TIP® Catheter, 1.4F, Single, Str., 15 cm, NR) was inserted to measure the RVSP and the systemic arterial pressure, respectively, as described previously (Janssen et al., 2015). After completion of data acquisition and haematocrit measurement, mice were exsanguinated under deep anaesthesia (5% isoflurane in oxygen supplement). In some cases, it was not possible to insert the catheter into the A. carotis, which is why there were only four mice in the PPE + L-NIL group.

2.6 | Haematocrit measurement

Immediately after haemodynamic measurements and the removal of the arterial catheter from the A. carotis, blood was collected using a capillary blood collection tube. Haematocrit was measured with a BAYER Rapidlab 348 RL Blood Gas Analyzer (Siemens Healthcare Diagnostics GmbH, Eschborn, Germany).

2.7 | Right ventricular hypertrophy

Hearts were removed and dissected into right ventricle (RV) and left ventricle plus septum (LV + S). RV hypertrophy was quantified by assessment of the Fulton Index (RV/(LV + S)).

2.8 | Lung fixation and processing

The lungs were flushed with saline through a cannula inserted into the pulmonary artery. Lungs (either left or right) were evenly allocated in the groups and used for alveolar/vascular morphometry as well as molecular investigations.

For molecular examinations, the lungs were snap frozen and stored at −80°C. For morphometry, fixation was performed for 20 min applying a 3.5%–3.7% formaldehyde solution through the trachea (fixation of alveoli) as well as the pulmonary artery (vascular perfusion) at 15- and 20-cmH_2O pressures respectively. The tracheal cannula was removed, and a surgical thread was tightened to ensure no leakage and to maintain the samples in an inflated state. Subsequently, the lungs were isolated and placed in formaldehyde overnight. The following day, the lungs were transferred to 0.1-M PBS. Afterwards, the lungs were embedded in agar and serially sectioned at 3-mm intervals using a special mould. The slices were then embedded in paraffin, and 3-μm sections were obtained using a microtome.

2.9 | Quantitative alveolar morphometry

For assessment of the mean linear intercept (MLI), the sections were cut (3 μm) from paraffin-embedded lungs and stained with haematoxylin and eosin. Scanning and analyses were performed by usage of Qwin software (Leica, Wetzlar, Germany) as described previously (Seimetz et al., 2011) by a blinded operator.

2.10 | Vascular morphometry

Sections of 3 μm thickness from paraffin-embedded lungs were used for the investigation. The lung slides were stained with antibodies against α-smooth muscle actin (α-SMA, violet; clone 1A4, Sigma-Aldrich, Munich, Germany, 1:900 dilution Sigma-Aldrich Cat# A2547, RRID:AB_476701) and von Willebrand factor (vWF, brown; Dako, Hamburg, Germany, 1:900 dilution Agilent Cat# A0082, RRID: AB_2315602) to quantify the degree of muscularization as follows: the percentage of α-SMA positive cells against the total vessel circumference was measured for every vessel and given as degree of muscularization using the Leica Qwin Software (Leica, Wetzlar, Germany). A total of 85 pulmonary vessels with a diameter of 20–70 μm were analysed, and the degree of muscularization from all 85 vessels was stated as mean muscularization of one mouse. Quantification was done by a blinded operator determining the mean muscularization of all counted vessels for every mouse and group as shown in Figures 2b and 4b. Additionally, numbers of vessels have been calculated manually for every left lung lobe of every mouse that was analysed for the degree of muscularization (Figure 7d) and sorted as either non-muscularized (without α-SMA staining, Figure 7e) or muscularized (with α-SMA staining, Figure 7f).

2.11 | Immunofluorescence staining for proliferating cell nuclear antigen (PCNA) and elastin

Paraffin sections of 3 μm thickness were de-paraffinized in xylol, rehydrated in serial washes with ethanol (100%, 90% and 70%) and finally washed in deionized water. Heat-mediated antigen retrieval (Tris-EDTA buffer, ph = 9) was performed, and the tissue was subsequently blocked in a blocking solution containing 5% BSA for 1 h at room temperature. Afterwards, the sections were incubated with primary antibodies overnight (4°C) and with secondary antibodies for 1 h in room temperature the following day. The blocking, antibody and washing solutions were prepared according to a previously published protocol (Rosas-Arellano et al., 2016). The antibodies used were Pro-

SPC (rabbit, dilution 1:1,000, Seven Hills Bioreagents Cat# WRAB-9337, RRID:AB_2335890), PCNA (mouse, dilution 1:200, Thermo Fisher Scientific Cat# 13-3900, RRID:AB_2533016), elastin (mouse, dilution 1:200, Santa Cruz Biotechnology Cat# sc-58756, RRID: AB_783200), anti-rabbit 647 (donkey, dilution 1:1,000, Molecular Probes Cat# A-31573, RRID:AB_2536183), anti-rabbit 488 (donkey, dilution 1:1,000) and anti-mouse 594 (donkey, dilution 1:1,000, Molecular Probes Cat# A-21203, RRID:AB_141633). After incubation with the secondary antibodies, the slides were washed and incubated for 1 h at room temperature with a conjugated α-sma-FITC (mouse, Sigma-Aldrich Cat# F3777, RRID:AB_476977) antibody. Nuclei were visualized with DAPI (4′,6-Diamidine-2′-phenylindole dihydrochloride) counterstaining (1:5,000). The slides were mounted with coverslips with Fluoromount W, and imaging was performed with a confocal microscope (Leica SP5, Leica, Wetzlar, Germany) with a 63× objective. As a first step, DAPI-stained nuclei and $PCNA^+$ cells were counted manually. Subsequently, $PCNA^+/SPC^+$ and $PCNA^+/\alpha\text{-sma}^+$ cells were manually counted as well. For the elastin quantification, the area occupied (pixels) by the fluorophore was measured using the software CellProfiler (CellProfiler Image Analysis Software, RRID:SCR_007358) with a script that initially applied the threshold function on the images (manually confirmed) and then the 'MeasureImageAreaOccupied' function to calculate the elastin content/field. To overcome the limitations presented by the discrepancies in tissue density between the group samples (control vs. L-NIL or placebo treated after elastase administration), the percentage of positive cells referring to the total number of cells per field from 10 random fields per lung was calculated. For the elastin quantification, a correction for tissue density was applied as described in the paragraph 'Connective tissue staining' (see below). The fields analysed were all from the alveolar compartment; fields with bigger airways were excluded from the measurements. The immuno-related procedures used comply with the recommendations made by the *British Journal of Pharmacology* (Alexander al., 2018).

2.12 | Staining for immune cells

Following the same protocol described above, immune cells were stained with a CD45 (rabbit, dilution 1:200, Abcam Cat# ab10558, RRID: AB_442810) and an anti-rabbit (donkey) antibody. Imaging was performed with a DM5500 B fluorescence microscope (Leica, Wetzlar, Germany). The percentage of $CD45^+$ cells was calculated as described above.

2.13 | Connective tissue staining (picro-sirius red staining)

For visualization of the connective tissue, slides were stained with picro-sirius red using a kit (Picro Sirius Red Stain Kit [Connective Tissue Stain], ab150681) according to the manufacturer's protocol. Briefly, the slides were de-paraffinized and hydrated in distilled water. They were incubated in picro-sirius red solution for 1 h, washed with acetic acid solution, cleared and mounted with PERTEX® mounting medium. The tissue was imaged with light microscopy and analysed using the Leica Qwin software with an appropriate—for this quantification—macro. The collagen area in % as calculated by the software was then corrected for the tissue density discrepancy as follows: an average of cell numbers (DAPI stained nuclei) per group (control, PPE + placebo, PPE + L-NIL) was calculated, and then a 'correction factor' (DAPI control:DAPI control, DAPI PPE + placebo:DAPI control, DAPI PPE + L-NIL:DAPI control) was used to normalize the collagen area in % for each individual measurement (correction factor of group × % of collagen area value) per tissue density of the corresponding group (nuclei number). Every value indicates the average of 25 images for each animal.

2.14 | Staining for Nitrotyrosine

Paraffin blocks were cut into 3-μm-thick slices and rehydrated. For antigen retrieval, slides were incubated in a pressure cooker for 45 min in rodent decloaker buffer (RD913, Biocare Medical, Pacheco, USA). Nitrotyrosine (3-NT) was stained overnight at +4°C using rabbit anti-nitrotyrosine antibody (N0409, Sigma-Aldrich, Munich, Germany, Sigma-Aldrich Cat# N0409, RRID:AB_260745) diluted 1:200 in a commercially available antibody diluent (ZUC025, Zytomed Systems GmbH). Afterwards, slides were incubated with Mouse/Rabbit alkaline phosphatase polymer kit (Zytomed Systems GmbH, Bargteheide, Germany) following the manufacturers recommendations. Staining was visualized using Warp red chromogen fluorescent kit (WR806, Biocare Medical, Pacheco, USA) following the manufacturers recommendations. Lung sections were counterstained with DAPI (1:1,000, Sigma-Aldrich, Munich, Germany) and covered with Dako fluorescent mounting medium. Slides were analysed the next day using a confocal microscope (Leica, Wetzlar, Germany). Nitrotyrosine was quantified as mean fluorescent intensity standardized to DAPI counterstaining, counted in five to 10 randomly selected fields per lung at 400× magnification.

2.15 | RNA extraction, cDNA synthesis and RT-PCR

An RNeasy Mini Kit (QIAGEN, Hilden, Germany) was used to extract the total mRNA from the mouse lung tissue according to the manufacturer's instructions following the iScript cDNA Synthesis Kit (BioRad, Munich, Germany) for PCR with reverse transcription of 1-μg RNA for every sample. The cycles for the reverse transcription were as follows: 1 cycle at 25°C for 5 min, 1 cycle at 46°C for 20 min and 1 cycle at 95°C for 1 min.

An iQ SYBR Green Supermix was used to perform real-time PCR according to the manufacturer's instructions (BioRad, Munich, Germany). The intron-spanning primers were designed by using the NCBI database and were as follows:

- PBGD_mouse_F: 5′-GGGAACCAGCTCTCTGAGGA-3′
- PBGD_mouse_R: 5′-GAATTCCTGCAGCTCATCCA-3′
- iNOS_mouse_F: 5′-ATGTGACATCGACCCGTCCAC-3′
- iNOS_mouse_R: 5′-GGGTAGGCTTGTCTCTGGGT-3′

The mRNA expression of iNOS was normalized to porphobilinogen deaminase (PBGD) and calculated using the ΔCt method.

2.16 | Western blot

Mice lungs were homogenized by Precellys® 24 bead beating Tissue Homogenizer (Bertin Corp, Thermo Fischer, Massachusetts, USA) in commercially available lysis buffer (#9803 Cell Signaling Technology, Massachusetts, USA) containing PMSF (1 mM). Lysates were separated on 10% or 12% polyacrylamide gels by electrophoresis (120 V, 400 mA, 150 W 1.5 h) and then transferred to a polyvinylidene difluoride (PVDF) membrane (Pall Corporation, Dreieich, Germany) using a semi-dry blotting system (Keutz, Germany). After blocking, the membranes were probed with one of the following primary antibodies: anti-HIF1α (1:1,000, Cayman Chemical, Ann Arbor, USA Cat# 10006421, RRID:AB_409037), anti-MMP8 (1:1,000, Abcam, Cambridge, UK, Cat# ab78423, RRID:AB_1566437), anti-MMP9 (1:1,000, Abcam, Cambridge, UK, Cat# ab38898, RRID:AB_776512), anti-MMP12 (1:1,000, Abcam, Cambridge, UK, Cat# ab52897, RRID:AB_2144836), anti-TNF-α (1:500, Santa Cruz Biotechnology, Texas, USA, Cat# sc-52746, RRID:AB_630341), anti-3-Nitrotyrosine (1:1,000, Abcam, Cambridge, UK, Cat# ab7048, RRID:AB_305725) and anti-β-actin (1:50,000, Abcam, Cambridge, UK, Cat# ab8226, RRID:AB_306371) overnight. Finally, the secondary antibody conjugated with HRP (anti-rabbit, Promega, Wisconsin, USA, Cat# W4011, RRID:AB_430833, anti-mouse, Promega, Wisconsin, USA, Cat# W4021, RRID:AB_430834) was applied for 1 h. The protein bands were visualized with the enhanced chemiluminescence solution kit (Clarity™, 1705061, Bio-Rad, California, USA), and the ChemiDoc MP Imaging System (17001402, Bio-Rad, California, USA) was employed for imaging. Densitometric analysis was calculated via Image Lab™ Software (Bio-Rad, California, USA), and expression was quantified using relative intensity ratio normalized to *β-actin*.

2.17 | Data and analysis

All data are shown in scatterplots and are stated as mean ± SEM. Numbers for every experiment (and group) are given in the figure legends and refer to the number of every individual mouse used in the respective group. Data obtained from inappropriate measurements (e.g., mouse dying during haemodynamic measurements, denaturation of protein and inappropriate melting curve) were excluded. Differences between the groups were assessed via weighted linear models (weighted ANOVA models). Weights were chosen to account to heteroscedasticity: animals treated with PPE generally showed a higher variance in all response values due to a heterogeneous reaction on the treatment. The weights were determined as the reciprocals of the variances of the residuals of a model including a factor specifying the PPE treatment (yes/no) besides the factor specifying the experimental group (some of which may be PPE treated). The analysis was checked by normal-quantile quantile plots and scale-location plots of the standardized residuals, which all looked reasonable. All data were analysed without any transformation except the data from area measurements, which were log-transformed. The specified linear hypothesis was tested only when the global model yielded $P < 0.05$. The reported P values are Holm-adjusted. Differences are considered statistically significant when adjusted p-values are lower than 0.05. Analyses were done using R (3.6.1; R Core Team, 2019) and the multcomp package (1.4–10; Hothorn, Bretz, & Westfall, 2008). Assessment of significance was only done for numbers ≥5 unless for the animal experiments, when only some groups had lower sample sizes (Figures 1 and 2a). The data and statistical analysis comply with the recommendations of the *British Journal of Pharmacology* on experimental design and analysis in pharmacology (Curtis et al., 2018).

2.18 | Nomenclature of targets and ligands

Key protein targets and ligands in this article are hyperlinked to corresponding entries in http://www.guidetopharmacology.org, the common portal for data from the IUPHAR/BPS Guide to PHARMACOLOGY (Harding et al., 2018), and are permanently archived in the Concise Guide to PHARMACOLOGY 2019/20 (Alexander et al., 2019).

3 | RESULTS

3.1 | A single-dose of porcine pancreatic elastase (PPE) instillation induces stable emphysema for 12 weeks

When compared to the control group, a single administration of PPE led to emphysema within 4 weeks after instillation, as indicated by the significant increase in both dynamic compliance (Figure 1a) and mean linear intercept (MLI; Figure 1b). Unless the compliance increased over time, these changes remained stable for up to 12 weeks post PPE administration (Figure 1a). Overview lung sections are given in Figure 1c

3.2 | Development of pulmonary hypertension and vascular remodelling after 12 weeks of PPE instillation

A one-time application of PPE induced pulmonary hypertension 12 weeks post instillation, as shown by an increased RVSP (Figure 2a) and an increased degree of muscularization (Figure 2b,c). The systemic BP (Figure S1A) and Fulton Index (Figure S1B) were unchanged.

3.3 | iNOS inhibition after establishment of elastase-induced emphysema improves lung structure and function

Next, we orally applied an iNOS inhibitor, L-NIL, starting treatment after established emphysema (Figure 3a). Both 3 and 15 weeks after PPE instillation, mice developed emphysema as demonstrated by the increased MLI, the dynamic compliance (Figure 3b,c) and the significantly decreased amount of elastin in the PPE + placebo group (Figure S4A,B). Treatment with L-NIL for 12 weeks resulted in a significant improvement of lung structure and function compared to the PPE + placebo group (Figures 3c,d and S4A,B). Overview lung sections are given in Figure 3d.

3.4 | iNOS inhibition after establishment of elastase-induced emphysema reverses pulmonary hypertension and vascular remodelling

Elastase induced pulmonary hypertension in the PPE-treated mice as indicated by a significant increased RVSP when compared to the control + placebo mice, whereas iNOS inhibition reversed PH (Figure 4a). The systemic arterial pressure remained unaltered, excluding a general effect of anaesthesia or L-NIL treatment on BP (Figure S1C). Assessment of Fulton Index revealed no differences between the groups (Figure S1D). Of interest, calculation of vessel numbers did not reveal significant changes after placebo or L-NIL treatment (Figure S1E). The changes in the RVSP are in line with the histological data where the increased muscularization in the PPE + placebo group returned to healthy conditions after L-NIL treatment (Figure 4b,d). Overview pictures of a fully and a non-muscularized vessel are given in Figure 4c.

3.5 | Effect of iNOS inhibition on nitrotyrosine expression, mRNA regulation and proliferation after emphysema development

To test the hypothesis that NOS-derived $ONOO^-$ formation provokes emphysema development and pulmonary hypertension by downstream signalling, we determined 3-nitrotyrosine as an indicator of $ONOO^-$ formation (Seimetz et al., 2011). Immunofluorescence staining targeting 3-nitrotyrosin demonstrated a significant up-regulation in the PPE + placebo group, which was completely reversed after L-NIL treatment (Figure 5a,b). These findings were supported by western blotting of lung homogenate, indicating a trend towards a reduction after L-NIL treatment (Figure S2A,B). Along these lines, expression levels of iNOS in lung homogenate were up-regulated in the elastase-induced mice but were fully restored after 12 weeks of L-NIL administration (Figure 5c).

Immunofluorescence staining for DAPI indicates a significant loss of cells after elastase instillation, which was significantly increased after L-NIL treatment (Figure S3A). Additionally, the proliferation marker PCNA was significantly increased after L-NIL treatment when compared to both the control and placebo-treated groups (Figure S3B). By allocation of PCNA fluorescence intensity to alveolar epithelial type II (ATII) cells and to smooth muscle actin (SMA) positive cells, an increase of alveolar epithelial type II and SMA^+ cells was detected after L-NIL treatment when compared to the control group (Figure 5d,e). In the L-NIL-treated group, almost 50% of the proliferating cells were positive for SPC, a marker of alveolar epithelial type II cells (Figure S3C), whereas only slightly changes in the amount of α-sma positive cells were visible between the groups (Figure S3C). Quantification of collagen indicated that there was no aberrant remodelling as there was no increase in collagen when comparing the L-NIL- to both placebo-treated groups (Figure S5A,B).

3.6 | Effect of iNOS inhibition on inflammation after emphysema development

To investigate the role of inflammatory cells in PPE-induced emphysema, we quantified immune cells ($CD45^+$). The lungs of the placebo-treated mice had a significantly higher percentage of immune cells per field, which was fully reversed in the L-NIL-treated mice (Figure 6a,b). Western blot analyses indicating the protein expression of different targets involved in inflammatory processes (TNF-α and MMPs 8, 9 and 12) were unchanged except for a significant increase in MMP12 after both placebo and L-NIL treatment (Figures 6c–f and S6A–D).

3.7 | Hypoxia does not drive the development of pulmonary hypertension in this elastase-induced mouse model

To answer the question whether hypoxia plays a role in the onset of pulmonary hypertension in our elastase model, we performed western blot analyses of **hypoxia inducible factor** (HIF)1α, which showed no regulation upon PPE application (Figure 7a,b). Along these lines, we measured the haematocrit (Figure 7c) of the placebo- or L-NIL-treated animals. There were no changes detectable between the three groups. Of interest, the total number of vessels over time was unchanged, although a trend towards a loss could be seen in the 12 weeks PPE group (Figure 7d). Moreover, a significant loss of non-muscularized vessels (vWF stained, Figure 7e) and a significantly increased number of muscularized vessels (α-SMA stained, Figure 7f) were visible 12 weeks post PPE instillation.

4 | DISCUSSION

Our data demonstrate that (i) a single intratracheal PPE administration leads to emphysema (after 3 weeks) and pulmonary hypertension (after 12 weeks) in mice, (ii) the degree of emphysema is stable over

12 weeks post instillation, which permits the investigation of pharmacological treatments, (iii) administration of the iNOS inhibitor L-NIL for 12 weeks improves emphysema and reverses pulmonary hypertension and (iv) iNOS-dependent signalling is involved in these processes.

Elastase application in mice is a well-characterized model of emphysema (Emami et al., 2008; Ishizawa et al., 2004; Lüthje et al., 2009; Munoz-Barrutia, Ceresa, Artaechevarria, Montuenga, & Ortiz-de-Solorzano, 2012; Snider, Lucey, & Stone, 1986; Suki, Bartolak-Suki, & Rocco, 2017; Valentine, Rucker, Chrisp, & Fisher, 1983) that has successfully been used to study pharmacological preventive (Takahashi et al., 2008; Tanaka et al., 2013) and curative (Padilha et al., 2015; Prakash Muyal, Kumar, Kotnala, Muyal, & Kumar Tyagi, 2015; Yildirim et al., 2010) treatments, yet no study utilizing an iNOS inhibitor in a treatment approach has been published so far. Elastase produces lesions in the lung, resulting in a more severe emphysema, than in the often-used tobacco smoke model. Moreover, it generates systemic effects similar to those seen in human COPD patients (Fournier & Lewis, 2000; Lüthje et al., 2009; Mattson, Sun, Murray, & Poole, 2002; Supinski & Kelsen, 1982), making it a very valuable screening technique for new interventions. PPE or human neutrophil elastase has been mainly used. PPE has the advantages of producing more consistent results, eastly obtainable and lastly, being less expensive than human neutrophil elastase (Antunes & Rocco, 2011). Different protocols exist, but a single elastase administration was shown to be sufficient to produce emphysema-like lesions within 21 days in mice (Ishizawa et al., 2004; Takahashi et al., 2008). This was confirmed in our study, where an intratracheal application of PPE resulted in emphysema as indicated by an increased pulmonary compliance 3 weeks post instillation.

However, this model has so far not been used for long-term curative investigations in emphysema. Therefore, we tested whether this type of induced emphysema is stable over a long period of time and thus would allow for testing of new pharmacological intervention and treatments. In this regard, we here have shown that the degree of emphysema is constant for at least 12 weeks after single PPE instillation. This was determined functionally by measuring dynamic compliance and structurally by MLI measurements at 4, 8 and 12 weeks after PPE application. Of note, a time-dependent increase in dynamic compliance, which was not connected to structural alterations, was observed and is in line with previous investigations in mice (Hirai et al., 1995) and humans (Lesauskaite & Ebejer, 1999; Meyer, 2005; Sharma & Goodwin, 2006). Importantly, the difference between every PPE and age-matched control groups was similar after 4, 8 and 12 weeks. We therefore conclude that our model produces stable and maintained emphysema. Intriguingly, this model provides a fast approach to generate severe emphysema, which is constant for at least 12 weeks, making it a very useful model for investigating new drug effects on this disease and mechanisms of lung regeneration in adult mice.

As demonstrated by others, prolonged emphysema was detectable in mice after 8 weeks (1.8 mg·kg^{-1} BW) (Otto-Verberne, Ten Have-Opbroek, Franken, Hermans, & Dijkman, 1992) and up to 161 days (80 units PPE·kg^{-1} BW) (Conlon et al., 2016) post PPE instillation and this is seen in hamsters after 120 days (4 units PPE per hamster) (Kleinerman, Ranga, Rynbrandt, Sorensen, & Powers, 1980) and upto 1 year (25 units per hamster) (Kuhn & Tavassoli, 1976). Furthermore, in these investigations have shown that the disease is progressive. This is a major difference between our study, where emphysema was stable for up to 12 weeks and could possibly be explained by species/strain-specific differences and the lower dose of PPE used in our study (24 units PPE·kg^{-1} BW).

In general, comparison between published elastase models is difficult, since not only the applied dose of elastase but also the way of administration (oropharyngeally, intranasally, orotracheally and intratracheally), the number of instillations (single vs. multiple) and the time between administration and examination (between hours and several weeks) varies. To the best of our knowledge, our model is the only one describing stable (persistent, not progressive) emphysema for up to 15 weeks (PPE + placebo) in mice after single-dose administration of PPE intratracheally.

Moreover, we have demonstrated that elastase instillation induces not only emphysema but also pulmonary hypertension. This was shown by the increased RVSP and the increased degree of lung vascular muscularization in those mice investigated 12 weeks after PPE application. Although these measurements clearly demonstrated the occurrence of pulmonary hypertension, we could not detect RV hypertrophy, indicating that the pulmonary hypertension is mild, it occurred 12 weeks after elastase application and was also not sufficient to induce RV remodelling. As RV hypertrophy in pulmonary hypertension is triggered by the increased afterload and the remodelling process requires time, this may well explain the absence of RV hypertrophy in our study and is in line with findings from other COPD-PH models, where RV hypertrophy occurs this only after the increase in RVSP has been established for some time (Seimetz et al., 2011). Interestingly, other studies failed to induce pulmonary hypertension, as indicated by the absence of vascular remodelling, RV hypertrophy and increased RVSP after one-time administration of elastase in mice (Lüthje et al., 2009; Suki et al., 2017). In contrast, we (in mice) and others (in hamsters [Fournier & Lewis, 2000; Mattson et al., 2002; Supinski & Kelsen, 1982]) could demonstrate an effect on the pulmonary circulation after elastase application. This discrepancy can be explained by the different time points of investigation after elastase application. Lüthje et al. (2009) examined mice after 3 weeks of instillation and Suki et al. (2017) between 2 days and 4 weeks, whereas Fournier, Mattson, and Supinski studied hamsters up to 18 months after elastase instillation (Fournier & Lewis, 2000; Mattson et al., 2002; Supinski & Kelsen, 1982). In summary, although other studies have already detected pulmonary hypertension after single administration of PPE in hamsters (e.g. Fournier & Lewis, 2000; Mattson et al., 2002; Supinski & Kelsen, 1982) or after multiple instillations in mice (e.g. Suki et al., 2017; de Novaes Rocha et al., 2017; Antunes et al., 2014; Lüthje et al., 2009), our model, to the best of our knowledge is the only one describing pulmonary hypertension in mice after single-dose administration of PPE intratracheally. Along these lines, we demonstrated that it takes at least

12 weeks until pulmonary hypertension is detectable when PPE is instilled once only. This is in contrast to, for example, tobacco smoke-induced emphysema in mice and guinea pigs where pulmonary hypertension develops prior to emphysema (Seimetz et al., 2011; Weissmann et al., 2014). The occurrence of pulmonary hypertension in a mouse model of elastase-induced emphysema has been described previously and can be explained by the destruction of the lung parenchyma combined with loss of capillaries, collagen deposition in the lung vasculature and increased intrathoracic pressure due to hyperinflation of the lung (Antunes & Rocco, 2011; Cruz et al., 2012; Oliveira et al., 2016).

In our model, neither hypoxia, as indicated by unchanged haematocrit and HIF1α expression, nor collagen deposition, as indicated by unaltered sirius-red staining, seems to be involved in the development of pulmonary hypertension. Of interest, it was demonstrated by Yu et al. (1998) that HIF1α protein expression in a ferret lung decreases within 1 min of reoxygenation. Therefore, the oxygen supplementation during haemodynamic measurements might alter the HIF1α expression in our model.

In line with the degree of muscularization, a significantly increase in the number of muscularized vessels, in addition to a significant loss of non-muscularized vessels were detectable 12 weeks post PPE instillation. This loss of vessels together with the alveolar destruction might limit the vascular reserve capacity and thus contribute, in addition to vascular remodelling, to an increased vascular resistance, but can also be a factor driving vascular remodelling due to increased blood flow/shear stress. This might drive the development of pulmonary hypertension, possibly in an iNOS-dependent fashion as suggested previously (Seimetz et al., 2011).

After successful establishment of the stable emphysema model, we, in the second part of our study, investigated the effect of the iNOS inhibitor L-NIL on established, severe emphysema and pulmonary hypertension. Most interestingly, we could demonstrate that iNOS is up-regulated upon elastase treatment, supporting the concept of iNOS as an important driver of emphysema development. This is supported by previous data from studies in smoke-exposed mice with mild emphysema (Seimetz et al., 2011). Boyer et al. (2011) also found a similar up-regulation of iNOS. Interestingly, in this study, iNOS inhibition had no preventive effect on emphysema development, which is in contrast to a study by Lanzetti et al. (2012) that found a protection from emphysema development in $iNOS^{-/-}$ mice. Such differences may be related to the 'aggressiveness' of the elastase applied, iNOS up-regulation may contribute to, but is not sufficient to induce emphysema alone if the 'digesting effect' of the elastase is quite high and overruns the iNOS effect. In line with this suggestion, Boyer et al. indeed used a higher dose of elastase than in our study, causing more severe lesions and destruction compared to our model (Mead, Turner, Macklem, & Little, 1967). Moreover, Boyer et al. investigated either $iNOS^{-/-}$ mice or WT mice treated with an iNOS inhibitor for up to 20 days after PPE instillation. In contrast, we applied an iNOS inhibitor for a much longer time period (12 weeks). Most likely, regeneration processes need more than 3 weeks to be detectable by significant changes in lung structure. These differences in study design may explain the above-mentioned differences.

Further to above studies we also investigated the lung regenerative capacity when iNOS was inhibited in our model. We found that pharmacological inhibition of iNOS triggers lung regenerative effects, as L-NIL treatment for 3 months was able to cause a significant improvement in the observed structural and functional deterioration of the lungs in this model. After L-NIL administration there was an increased proliferation as indicated by the rising number of PCNA-positive cells, predominately alveolar epithelial type II cells, which most likely triggered this regeneration. Alveolar epithelial type II cells have been demonstrated to renew the alveolar epithelial population in the steady state condition and to have regenerative capacity after injury (Barkauskas et al., 2013). Moreover, staining for proliferating myofibroblasts ($PCNA^{+}\alpha\text{-}sma^{+}$) indicated that, although these cells are significantly increased after L-NIL treatment, they were barely represented (≈0.28% of total cells) in the L-NIL-treated group. Additionally, the significantly lower collagen content in the L-NIL- and placebo-treated mice compared to the control indicated the absence of fibrosis and thus aberrant remodelling. Finally, immune cell numbers ($CD45^{+}$) were significantly increased after PPE instillation and restored to baseline level after L-NIL treatment. This is in line with the positive effect of L-NIL treatment on the lung structure, although we could only detect changes in protein expression targeting **MMP12** and not in other proteins related to inflammatory processes (**TNF-α**, **MMP8** and **MMP9**). This can be explained by the late time point (15 weeks after PPE instillation) of our analysis: It is known that inflammation in elastase-induced emphysema is an acute feature (Couillin et al., 2009; Vidal et al., 2012), where inflammatory markers are up-regulated early after elastase administration. Thus, it has been shown by Kurimoto et al. (2013) that **IL-17A** is only up-regulated during the first 2 days after elastase application. Of interest, MMP12 remains up-regulated after L-NIL treatment. A possible explanation for this finding might be that we have investigated lung homogenate and therefore, possibly have missed the down-regulation of MMP12 in specific cells (alveolar epithelial type II cells) after L-NIL application. Finally, it could be due to different mechanisms that drive emphysema development/regeneration and that MMP12 is not involved in these regeneration processes.

Overall, these data suggest that our model indeed shows partial regeneration of the lung parenchyma after L-NIL treatment and not aberrant remodelling. The sustained up-regulation of MMP12 after L-NIL administration might explain why we only could see partial reversal of emphysema, since both beneficial (down-regulation of iNOS, nitrotyrosine, decrease in immune cell numbers) and emphysema-driving pathways (up-regulation of MMP12) seem to be activated at the same time. The persistent emphysema in the placebo group could potentially be attributed to the higher number of immune cells, residing in the alveolar compartment long after the injury induced by PPE instillation.

Concerning pulmonary hypertension, L-NIL application for 12 weeks elicited not only a reversal of the RVSP back to health conditions but also a reduced muscularization, when compared to the

placebo-treated mice. Thus, L-NIL treatment did not only improve emphysema but also reverse the elastase-induced pulmonary vascular phenotype, including pulmonary hypertension. In this regard it is important to mention that the occurrence of even mild pulmonary hypertension reduces the survival of COPD patients (Elwing & Panos, 2008). Of interest, Fulton Index, a measure of RV hypertrophy, was not significantly increased in the placebo-treated mice, which is in line with our finding that the mild pulmonary hypertension, 12 weeks after elastase application, was not sufficient to induce RV remodelling.

It was demonstrated by our group, as well as by others, that nitrosative/oxidative stress produced by NO plays a pivotal role during establishment of emphysema (Lanzetti et al., 2012) and pulmonary hypertension (Seimetz et al., 2011). NO produced excessively by iNOS rapidly reacts with superoxide released from different cell types (e.g. inflammatory cells) and leads to the production of reactive nitrogen species (RNS) and most importantly peroxynitrite, which is highly pro-inflammatory and can alter protein function (Bartesaghi & Radi, 2018; Beckman et al., 1990; Hensley et al., 1998; Pryor & Squadrito, 1995; Radi, 2013). In contrast to superoxide, peroxynitrite is a slow reacting agent with a high diffusional capacity, causing selective cytotoxic effects (Szabo, Ischiropoulos, & Radi, 2007). Peroxynitrite can inactivate anti-proteases (Whiteman & Halliwell, 1997) and activate matrix-metalloproteinases (Okamoto et al., 2001), enzymes involved in both emphysema (Houghton, 2015) and pulmonary hypertension development (Chelladurai, Seeger, & Pullamsetti, 2012). Furthermore, the crucial role of oxidative/nitrosative stress during development of elastase-induced emphysema has already been demonstrated and was accompanied with increased nitrotyrosine levels (Boyer et al., 2011). Although our western blot analysis showed no significant regulation when analysing whole lung homogenate, an immunofluorescence staining targeting 3-nitrotyrosine demonstrated a significant up-regulation in the placebo-treated group, which was completely reversed following L-NIL treatment. The reduction of 3-nitrotyrosine in the lungs after L-NIL treatment and the increased level in the placebo group provides evidence that L-NIL is able to antagonize lung parenchyma damage by restoring the oxidant/antioxidant balance.

Our study provides certain advantages by demonstrating that (i) a low-dose instillation of elastase results in stable emphysema and (ii) this single instillation is able to generate pulmonary hypertension. Nevertheless, our study has two major limitations. The first, we have used a mouse model generating acute emphysema, which is not able to reproduce all features of chronic emphysema in humans. Therefore, this model is not suitable to investigate development and consequently the patho-mechanisms leading to human emphysema. Our intention, however, is to use it as a rather fast model to investigate the impact of pharmacological treatment for lung regeneration that is targeting both alveolar destruction and vascular remodelling. The second is that caution should be observed in transferring findings from mice to human lung emphysema/COPD-PH. Nevertheless, we are convinced that our model and results might be helpful to screen possible new drugs in a preclinical model and, therefore, help to develop treatments for human COPD.

In conclusion, our data demonstrate the establishment of a model of severe emphysema in mice allows the investigation of different possible pharmacological treatments. We demonstrated that pharmacological inhibition of iNOS by oral application is able to improve severe, elastase-induced emphysema and to reverse the accompanying pulmonary hypertension. The present study thus provides further evidence for iNOS inhibition as a treatment of lung emphysema. Further studies need to be carried out to confirm if this target can be used in the treatment of the human disease.

ACKNOWLEDGEMENT

The authors would like to thank Dr. Clemens Ruppert, Ewa Bieniek, Karin Quanz and Ingrid Breitenborn-Müller for technical assistance. This work was funded by the Deutsche Forschungsgemeinschaft (DFG, German Research Foundation)—project number 268555672—SFB 1213, project A07.

AUTHOR CONTRIBUTIONS

A.F., M.S., H.A.G., M.G., R.T.S., W.S., F.G., N.W. and SK designed the study. Data were acquired by A.F., S.H., C.-Y.W., K.M., A.P., M.B., and E.T.R. and analysed as well as interpreted by A.F., S.H., F.K., C-.Y.W., K.M., J.W., A.P., M.B., E.T.R. and S.K. The manuscript was drafted by A.F., F.K. and S.K. and revised by M.S., S.H., C-.Y.W., K.M., J.W., A.P., M.B., E.T.R., H.A.G., N.S., M.G., R.T.S., W.S., F.G. and N.W.

CONFLICT OF INTEREST

The authors declare no conflicts of interest.

DECLARATION OF TRANSPARENCY AND SCIENTIFIC RIGOUR

This Declaration acknowledges that this paper adheres to the principles for transparent reporting and scientific rigour of preclinical research as stated in the BJP guidelines for Design & Analysis, Immunoblotting and Immunochemistry and Animal Experimentation, and as recommended by funding agencies, publishers and other organisations engaged with supporting research.

REFERENCES

Alexander, S. P. H., Roberts, R. E., Broughton, B. R. S., Sobey, S. G., George, C. H., Stanford, S. C., … Ahluwalia, A. (2018). Goals and practicalities of immunoblotting and immunohistochemistry: A guide for submission to the British Journal of Pharmacology. *British journal of pharmacology*, *175*, 407–411. https://doi.org/10.1111/bph.14112

Alexander, S. P. H., Fabbro, D., Kelly, E., Mathie, A., Peters, J. A., Veale, E. L., … Sharman, J. L. (2019). THE CONCISE GUIDE TO PHARMACOLOGY 2019/20: Enzymes. *British Journal of Pharmacology*, *176*, S297–S396.

Antunes, M. A., Abreu, S. C., Cruz, F. F., Teixeira, A. C., Lopes-Pacheco, M., Bandeira, E., … Rocco, P. R. M. (2014). Effects of different mesenchymal stromal cell sources and delivery routes in experimental emphysema. *Respiratory Research*, *15*, 118. https://doi.org/10.1186/s12931-014-0118-x

Antunes, M. A., & Rocco, P. R. (2011). Elastase-induced pulmonary emphysema: insights from experimental models. *Anais da Academia Brasileira de Ciências*, *83*, 1385–1396. https://doi.org/10.1590/s0001-37652011005000039

Barkauskas, C. E., Cronce, M. J., Rackley, C. R., Bowie, E. J., Keene, D. R., Stripp, B. R., … Hogan, B. L. (2013). Type 2 alveolar cells are stem cells in adult lung. *The Journal of Clinical Investigation*, *123*, 3025–3036. https://doi.org/10.1172/JCI68782

Bartesaghi, S., & Radi, R. (2018). Fundamentals on the biochemistry of peroxynitrite and protein tyrosine nitration. *Redox Biology*, *14*, 618–625.

Beckman, J. S., Beckman, T. W., Chen, J., Marshall, P. A., & Freeman, B. A. (1990). Apparent hydroxyl radical production by peroxynitrite: implications for endothelial injury from nitric oxide and superoxide. *Proceedings of the National Academy of Sciences of the United States of America*, *87*, 1620–1624. https://doi.org/10.1073/pnas.87.4.1620

Bohadana, A. B., Nilsson, F., Westin, A., Martinet, N., & Martinet, Y. (2006). Smoking cessation--but not smoking reduction--improves the annual decline in FEV1 in occupationally exposed workers. *Respiratory Medicine*, *100*, 1423–1430. https://doi.org/10.1016/j.rmed.2005.11.005

Boyer, L., Plantier, L., Dagouassat, M., Lanone, S., Goven, D., Caramelle, P., … Boczkowski, J. (2011). Role of nitric oxide synthases in elastase-induced emphysema. *Laboratory Investigation*, *91*, 353–362. https://doi.org/10.1038/labinvest.2010.169

Cazzola, M., Donner, C. F., & Hanania, N. A. (2007). One hundred years of chronic obstructive pulmonary disease (COPD). *Respiratory Medicine*, *101*, 1049–1065. https://doi.org/10.1016/j.rmed.2007.01.015

Chelladurai, P., Seeger, W., & Pullamsetti, S. S. (2012). Matrix metalloproteinases and their inhibitors in pulmonary hypertension. *The European Respiratory Journal*, *40*, 766–782. https://doi.org/10.1183/09031936.00209911

Conlon, T. M., Bartel, J., Ballweg, K., Gunter, S., Prehn, C., Krumsiek, J., … Yildirim, A. Ö. (2016). Metabolomics screening identifies reduced L-carnitine to be associated with progressive emphysema. *Clinical Science (London, England)*, *130*, 273–287. https://doi.org/10.1042/CS20150438

Couillin, I., Vasseur, V., Charron, S., Gasse, P., Tavernier, M., Guillet, J., … Ryffel, B. (2009). IL-1R1/MyD88 signaling is critical for elastase-induced lung inflammation and emphysema. *Journal of Immunology*, *183*, 8195–8202. https://doi.org/10.4049/jimmunol.0803154

Cruz, F. F., Antunes, M. A., Abreu, S. C., Fujisaki, L. C., Silva, J. D., Xisto, D. G., … Rocco, P. R. (2012). Protective effects of bone marrow mononuclear cell therapy on lung and heart in an elastase-induced emphysema model. *Respiratory Physiology & Neurobiology*, *182*, 26–36. https://doi.org/10.1016/j.resp.2012.01.002

Curtis, M. J., Alexander, S., Cirino, G., Docherty, J. R., George, G. H., Giembycz, M. A., et al. (2018). Experimental design and analysis and their reporting II: updated and simplified guidance for authors and peer reviewers. *British Journal of Pharmacology*, *175*(7), 987–993. https://doi.org/10.1111/bph.14153

de Novaes Rocha, N., de Oliveira, M. V., Braga, C. L., Guimaraes, G., de Albuquerque Maia, L., de Araújo Padilha, G., … Rocco, P. R. (2017). Ghrelin therapy improves lung and cardiovascular function in experimental emphysema. *Respiratory Research*, *18*, 185. https://doi.org/10.1186/s12931-017-0668-9

Dijkstra, G., Moshage, H., van Dullemen, H. M., de Jager-Krikken, A., Tiebosch, A. T., Kleibeuker, J. H., … van Goor, H. (1998). Expression of nitric oxide synthases and formation of nitrotyrosine and reactive oxygen species in inflammatory bowel disease. *The Journal of Pathology*, *186*, 416–421. https://doi.org/10.1002/(SICI)1096-9896(199812)186:4<416::AID-PATH201>3.0.CO;2-U

Elwing, J., & Panos, R. J. (2008). Pulmonary hypertension associated with COPD. *International Journal of Chronic Obstructive Pulmonary Disease*, *3*, 55–70.

Emami, K., Cadman, R. V., Woodburn, J. M., Fischer, M. C., Kadlecek, S. J., Zhu, J., … Friscia, M. E. (2008). Early changes of lung function and structure in an elastase model of emphysema—A hyperpolarized 3He MRI study. *Journal of Applied Physiology*, *104*, 773–786.

Fournier, M., & Lewis, M. I. (2000). Functional, cellular, and biochemical adaptations to elastase-induced emphysema in hamster medial scalene. *Journal of Applied Physiology*, *88*, 1327–1337.

Girard, A., Jouneau, S., Chabanne, C., Khouatra, C., Lannes, M., Traclet, J., … Cottin, V. (2015). Severe pulmonary hypertension associated with COPD: hemodynamic improvement with specific therapy. *Respiration*, *90*, 220–228. https://doi.org/10.1159/000431380

Harding, S. D., Sharman, J. L., Faccenda, E., Southan, C., Pawson, A. J., Ireland, S., … NC-IUPHAR. (2018). The IUPHAR/BPS Guide to PHARMACOLOGY in 2018: updates and expansion to encompass the new guide to IMMUNOPHARMACOLOGY. *Nucleic Acids Research*, *46*, D1091–d1106. https://doi.org/10.1093/nar/gkx1121

Hensley, K., Maidt, M. L., Yu, Z., Sang, H., Markesbery, W. R., & Floyd, R. A. (1998). Electrochemical analysis of protein nitrotyrosine and dityrosine in the Alzheimer brain indicates region-specific accumulation. *The Journal of Neuroscience*, *18*, 8126–8132.

Hirai, T., Hosokawa, M., Kawakami, K., Takubo, Y., Sakai, N., Oku, Y., … Kuno, K. (1995). Age-related changes in the static and dynamic mechanical properties of mouse lungs. *Respiration Physiology*, *102*, 195–203. https://doi.org/10.1016/0034-5687(95)00068-2

Hothorn, T., Bretz, F., & Westfall, P. (2008). Simultaneous Inference in general parametric models. *Biometrical Journal*, *50*, 346–363. https://doi.org/10.1002/bimj.200810425

Houghton, A. M. (2015). Matrix metalloproteinases in destructive lung disease. *Matrix Biology*, *44-46*, 167–174. https://doi.org/10.1016/j.matbio.2015.02.002

Ishizawa, K., Kubo, H., Yamada, M., Kobayashi, S., Numasaki, M., Ueda, S., … Sasaki, H. (2004). Bone marrow-derived cells contribute to lung regeneration after elastase-induced pulmonary emphysema. *FEBS Letters*, *556*, 249–252. https://doi.org/10.1016/s0014-5793(03)01399-1

Janssen, W., Schymura, Y., Novoyatleva, T., Kojonazarov, B., Boehm, M., Wietelmann, A., … Pullamsetti, S. S. (2015). 5-HT2B Receptor Antagonists Inhibit Fibrosis and Protect from RV Heart Failure. *BioMed Research*, *2015*, 438403, 8 pages. https://doi.org/10.1155/2015/438403

Kankaanranta, H., Harju, T., Kilpeläinen, M., Mazur, W., Lehto, J. T., Katajisto, M., … Lehtimäki, L. (2015). Diagnosis and Pharmacotherapy of Stable Chronic Obstructive Pulmonary Disease: The Finnish Guidelines. *Basic & Clinical Pharmacology & Toxicology*, *116*, 291–307. https://doi.org/10.1111/bcpt.12366

Kilkenny, C., Browne, W., Cuthill, I. C., Emerson, M., & Altman, D. G. (2010). Animal research: Reporting *in vivo* experiments: the ARRIVE guidelines. *British Journal of Pharmacology*, *160*, 1577–1579.

Kleinerman, J., Ranga, V., Rynbrandt, D., Sorensen, J., & Powers, J. C. (1980). The effect of the specific elastase inhibitor, alanyl prolyl alanine chloromethylketone, on elastase-induced emphysema. *The American Review of Respiratory Disease*, *121*, 381–387. https://doi.org/10.1164/arrd.1980.121.2.381

Kuhn, C. 3rd, & Tavassoli, F. (1976). The scanning electron microscopy of elastase-induced emphysema. A comparison with emphysema in man. *Laboratory Investigation*, *34*, 2–9.

Kurimoto, E., Miyahara, N., Kanehiro, A., Waseda, K., Taniguchi, A., Ikeda, G., … Tanimoto, M. (2013). IL-17A is essential to the development of elastase-induced pulmonary inflammation and emphysema in mice. *Respiratory Research*, *14*, 5. https://doi.org/10.1186/1465-9921-14-5

Lanzetti, M., da Costa, C. A., Nesi, R. T., Barroso, M. V., Martins, V., Victoni, T., … Valença, S. S. (2012). Oxidative stress and nitrosative stress are involved in different stages of proteolytic pulmonary emphysema. *Free Radical Biology & Medicine*, *53*, 1993–2001. https://doi.org/10.1016/j.freeradbiomed.2012.09.015

Lesauskaite, V., & Ebejer, M. J. (1999). Age-Related Changes in the Respiratory System. *Maltese Medical Journal*, *11*, 25–30.

Lüthje, L., Raupach, T., Michels, H., Unsöld, B., Hasenfuss, G., Kögler, H., & Andreas, S. (2009). Exercise intolerance and systemic manifestations of pulmonary emphysema in a mouse model. *Respiratory Research*, *10*, 7–7. https://doi.org/10.1186/1465-9921-10-7

Mattson, J. P., Sun, J., Murray, D. M., & Poole, D. C. (2002). Lipid peroxidation in the skeletal muscle of hamsters with emphysema. *Pathophysiology*, *8*, 215–221. https://doi.org/10.1016/s0928-4680(02)00011-1

Mead, J., Turner, J. M., Macklem, P. T., & Little, J. B. (1967). Significance of the relationship between lung recoil and maximum expiratory flow. *Journal of Applied Physiology*, *22*, 95–108. https://doi.org/10.1152/jappl.1967.22.1.95

Meyer, K. C. (2005). Aging. *Proceedings of the American Thoracic Society*, *2*, 433–439.

Minai, O. A., Chaouat, A., & Adnot, S. (2010). Pulmonary hypertension in COPD: epidemiology, significance, and management: pulmonary vascular disease: the global perspective. *Chest*, *137*, 39s–51s.

Munoz-Barrutia, A., Ceresa, M., Artaechevarria, X., Montuenga, L. M., & Ortiz-de-Solorzano, C. (2012). Quantification of lung damage in an elastase-induced mouse model of emphysema. *International Journal of Biomedical Imaging*, *2012*, 734734.

Okamoto, T., Akaike, T., Sawa, T., Miyamoto, Y., van der Vliet, A., & Maeda, H. (2001). Activation of matrix metalloproteinases by peroxynitrite-induced protein S-glutathiolation via disulfide S-oxide formation. *The Journal of Biological Chemistry*, *276*, 29596–29602. https://doi.org/10.1074/jbc.M102417200

Oliveira, M. V., Abreu, S. C., Padilha, G. A., Rocha, N. N., Maia, L. A., Takiya, C. M., … Rocco, P. R. (2016). Characterization of a Mouse Model of Emphysema Induced by Multiple Instillations of Low-Dose Elastase. *Frontiers in Physiology*, *7*, 457.

Otto-Verberne, C. J., Ten Have-Opbroek, A. A., Franken, C., Hermans, J., & Dijkman, J. H. (1992). Protective effect of pulmonary surfactant on elastase-induced emphysema in mice. *The European Respiratory Journal*, *5*, 1223–1230.

Padilha, G. A., Henriques, I., Lopes-Pacheco, M., Abreu, S. C., Oliveira, M. V., Morales, M. M., … Rocco, P. R. (2015). Therapeutic effects of LASSBio-596 in an elastase-induced mouse model of emphysema. *Frontiers in Physiology*, *6*, 267.

Prakash Muyal, J., Kumar, D., Kotnala, S., Muyal, V., & Kumar Tyagi, A. (2015). Recombinant Human Keratinocyte Growth Factor Induces Akt Mediated Cell Survival Progression in Emphysematous Mice. *Archivos de Bronconeumología*, *51*, 328–337. https://doi.org/10.1016/j.arbres.2014.04.019

Pryor, W. A., & Squadrito, G. L. (1995). The chemistry of peroxynitrite: a product from the reaction of nitric oxide with superoxide. *The American Journal of Physiology*, *268*, L699–L722.

Radi, R. (2013). Peroxynitrite, a stealthy biological oxidant. *The Journal of Biological Chemistry*, *288*, 26464–26472.

R Core Team. (2019). R: A language and environment for statistical computing. R foundation for statistical computing, Vienna, Austria. URL https://www.R-project.org/

Rosas-Arellano, A., Villalobos-Gonzalez, J. B., Palma-Tirado, L., Beltran, F. A., Carabez-Trejo, A., Missirlis, F., & Castro, M. A. (2016). A simple solution for antibody signal enhancement in immunofluorescence and triple immunogold assays. *Histochemistry and Cell Biology*, *146*, 421–430. https://doi.org/10.1007/s00418-016-1447-2

Russell, W. M. S., & Burch, R. L. (1959). *The Principles of Humane Experimental Technique*. Methuen: Methuen Publishing.

Sangani, R. G., & Ghio, A. J. (2011). Lung injury after cigarette smoking is particle related. *International Journal of Chronic Obstructive Pulmonary Disease*, *6*, 191–198. https://doi.org/10.2147/COPD.S14911

Seimetz, M., Parajuli, N., Pichl, A., Veit, F., Kwapiszewska, G., Weisel, F. C., … Weissmann, N. (2011). Inducible NOS inhibition reverses tobacco-smoke-induced emphysema and pulmonary hypertension in mice. *Cell*, *147*, 293–305. https://doi.org/10.1016/j.cell.2011.08.035

Sharma, G., & Goodwin, J. (2006). Effect of aging on respiratory system physiology and immunology. *Clinical Interventions in Aging*, *1*, 253–260. https://doi.org/10.2147/ciia.2006.1.3.253

Snider, G. L., Kleinerman, J., Thurlbeck, W. M., & Bengali, Z. (1985). The definition of emphysema. Report of a National Heart, Lung, and Blood Institute, Division of Lung Diseases workshop. *The American Review of Respiratory Disease*, *132*, 182–185.

Snider, G. L., Lucey, E. C., & Stone, P. J. (1986). Animal models of emphysema. *The American Review of Respiratory Disease*, *133*, 149–169. https://doi.org/10.1164/arrd.1986.133.1.149

Stenger, S., Thuring, H., Rollinghoff, M., Manning, P., & Bogdan, C. (1995). L-N6-(1-iminoethyl)-lysine potently inhibits inducible nitric oxide synthase and is superior to NG-monomethyl-arginine in vitro and in vivo. *European Journal of Pharmacology*, *294*, 703–712. https://doi.org/10.1016/0014-2999(95)00618-4

Suki, B., Bartolak-Suki, E., & Rocco, P. R. M. (2017). Elastase-Induced Lung Emphysema Models in Mice. *Methods in Molecular Biology*, *1639*, 67–75. https://doi.org/10.1007/978-1-4939-7163-3_7

Supinski, G. S., & Kelsen, S. G. (1982). Effect of elastase-induced emphysema on the force-generating ability of the diaphragm. *The Journal of Clinical Investigation*, *70*, 978–988. https://doi.org/10.1172/jci110709

Szabo, C., Ischiropoulos, H., & Radi, R. (2007). Peroxynitrite: biochemistry, pathophysiology and development of therapeutics. *Nature Reviews. Drug Discovery*, *6*, 662–680. https://doi.org/10.1038/nrd2222

Takahashi, S., Nakamura, H., Seki, M., Shiraishi, Y., Yamamoto, M., Furuuchi, M., … Ishizaka, A. (2008). Reversal of elastase-induced pulmonary emphysema and promotion of alveolar epithelial cell proliferation by simvastatin in mice. *American Journal of Physiology. Lung Cellular and Molecular Physiology*, *294*, L882–L890. https://doi.org/10.1152/ajplung.00238.2007

Tanaka, K., Ishihara, T., Sugizaki, T., Kobayashi, D., Yamashita, Y., Tahara, K., … Sato, K. (2013). Mepenzolate bromide displays beneficial effects in a mouse model of chronic obstructive pulmonary disease. *Nature Communications*, *4*, 2686. https://doi.org/10.1038/ncomms3686

Valentine, R., Rucker, R. B., Chrisp, C. E., & Fisher, G. L. (1983). Morphological and biochemical features of elastase-induced emphysema in strain A/J mice. *Toxicology and Applied Pharmacology*, *68*, 451–461. https://doi.org/10.1016/0041-008x(83)90290-9

Vidal, D., Fortunato, G., Klein, W., Cortizo, L., Vasconcelos, J., Ribeiro-Dos-Santos, R., … Macambira, S. (2012). Alterations in pulmonary structure by elastase administration in a model of emphysema in mice is associated with functional disturbances. *Revista Portuguesa de Pneumologia*, *18*, 128–136. https://doi.org/10.1016/j.rppneu.2011.12.007

Weissmann, N., Lobo, B., Pichl, A., Parajuli, N., Seimetz, M., Puig-Pey, R., … Barberà, J. A. (2014). Stimulation of soluble guanylate cyclase prevents cigarette smoke-induced pulmonary hypertension and emphysema. *American Journal of Respiratory and Critical Care Medicine*, *189*, 1359–1373. https://doi.org/10.1164/rccm.201311-2037OC

Whiteman, M., & Halliwell, B. (1997). Prevention of peroxynitrite-dependent tyrosine nitration and inactivation of alpha1-antiproteinase by antibiotics. *Free Radical Research*, *26*, 49–56. https://doi.org/10.3109/10715769709097783

Yildirim, A. O., Muyal, V., John, G., Muller, B., Seifart, C., Kasper, M., & Fehrenbach, H. (2010). Palifermin induces alveolar maintenance programs in emphysematous mice. *American Journal of Respiratory and Critical Care Medicine*, *181*, 705–717. https://doi.org/10.1164/rccm.200804-573OC

Yu, A. Y., Frid, M. G., Shimoda, L. A., Wiener, C. M., Stenmark, K., & Semenza, G. L. (1998). Temporal, spatial, and oxygen-regulated expression of hypoxia-inducible factor-1 in the lung. *The American Journal of Physiology*, *275*, L818–L826. https://doi.org/10.1152/ajplung.1998.275.4.L818

SUPPORTING INFORMATION

Additional supporting information may be found online in the Supporting Information section at the end of this article.

How to cite this article: Fysikopoulos A, Seimetz M, Hadzic S, et al. Amelioration of elastase-induced lung emphysema and reversal of pulmonary hypertension by pharmacological iNOS inhibition in mice. *Br J Pharmacol*. 2021;178:152–171. https://doi.org/10.1111/bph.15057